Engineering Fracture Mechanics Vol. 21, No. 2, pp. 341–351, 1985
Printed in the U.S.A.

0013-7944/85 $3.00 + .00
Pergamon Press Ltd.

# DIRECTIONAL EFFECTS IN ASYMMETRIC FULLY PLASTIC CRACK GROWTH

G. A. KARDOMATEAS, F. A. McCLINTOCK and W. T. CARTER
Massachusetts Institute of Technology, Cambridge, MA 02139, U.S.A.

**Abstract**—Asymmetrically cracked specimens fail with considerably less ductility than symmetrically cracked ones. Indeed, welds, shoulders or other asymmetries may eliminate one of the shear bands and thus result in crack propagation through predamaged material instead of the relatively unstrained region between two plastic shear zones of the symmetric case. An incremental approach is presented for predicting the direction of the growing crack and the crack growth conditions (far field displacement, strain, triaxiality). The formulation is based on strain increments following a power law relation and on the hole growth fracture criterion of McClintock, Kaplan and Berg [5]. At each step several sites are considered ahead of the crack and the damage due to crack initiation and prior growth is calculated. The crack is assumed to advance to the direction that requires the minimum far field displacement to reach critical damage. The predicted displacement to crack initiation is found to be of the order of the critical strain times the mean inclusion spacing. Results for two strain hardening exponents $n = \frac{1}{4}$ and $n = \frac{1}{15}$ and several initial crack-shear band angles are presented. In general the crack does not progress along the shear band but at an angle of 23°–32° giving a higher triaxiality. Strain hardening affects the rate of crack advance per unit displacement and the critical growth strain as well as the final crack orientation. The overall computer program provides a quick and direct approach that enables estimating the failure conditions of asymmetrically cracked structures from material data.

## INTRODUCTION

MOST FRACTURE tests use symmetric specimens. The crack advances into relatively undamaged material between two shear bands. This may not happen, however, if one of the bands is eliminated due to a weld, for example, or a harder heat-affected zone (Fig. 1). A fatigue crack or some other defect near such an asymmetry will find only one shear band and, as a consequence, will advance through highly strained material. Lower ductility is thus expected. The formation of a shear lip at the end of an ordinary cup and cone fracture in a tensile test (McClintock and David [4]) supports this fact. Asymmetric crack analysis will become increasingly important as fully-plastic fracture mechanics finds its way into the design of ductile structures with welds or other abrupt changes in geometry.

McClintock and Slocum [6] developed a formulation for the accumulation of damage ahead of the crack in a power-law strain hardening material, by assuming that the crack advances directly along the shear band. Preliminary experiments, however, have indicated that the crack actually advances at an angle from the shear band.

In the following we present an incremental solution for the growing crack by using the strain and displacement fields derived by Shih [7] for a stationary mixed Mode crack. After accumulating damage from prior growth, the necessary far-field displacement to cause crack growth in each direction is found by using the McClintock, Kaplan and Berg [5] hole growth criterion. The crack is assumed to advance in the direction requiring the least far-field displacement.

## ANALYSIS

A solution for the small scale yielding of mixed Modes I and II stationary crack problems has been developed by Shih [7]. The material was assumed to be power-law hardening according to the constitutive relation between equivalent stress and strain:

$$\sigma = \bar{\sigma}_1 \epsilon^n \tag{1}$$

where $\bar{\sigma}_1$ is the flow stress at unit strain and $n$ is the strain hardening exponent. A mixity

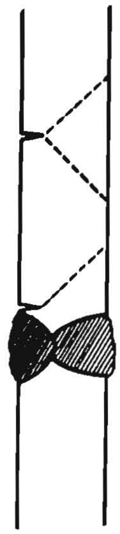

Fig. 1. Asymmetric crack from a defect near a weld; the symmetric case is shown above.

parameter $M^p$ was introduced, defined in terms of the near field stresses by:

$$M^p = \frac{2}{\pi}\tan^{-1}\left|\lim_{r\to 0}\frac{\sigma_{\theta\theta}(r, \theta = 0)}{\sigma_{r\theta}(r, \theta = 0)}\right|. \tag{2}$$

Thus the mixity parameter varies from 0 for pure Mode II to 1 for pure Mode I. McClintock [3] restated the dominant singularity governing the behavior of the stresses, strains and displacements in terms of the $J$ integral as:

$$\begin{aligned}
\frac{\sigma_{ij}}{\bar{\sigma}_1} &= \left[\frac{J}{\bar{\sigma}_1 r\, I(n, M^p)}\right]^{n/(n-1)} \tilde{\sigma}_{ij}(\theta, M^p, n),\\
\epsilon_{ij} &= \left[\frac{J}{\bar{\sigma}_1 r\, I(n, M^p)}\right]^{1/(n-1)} \tilde{\epsilon}_{ij}(\theta, M^p, n),\\
\frac{u_i}{r} &= \left[\frac{J}{\bar{\sigma}_1 r\, I(n, M^p)}\right]^{1/(n-1)} \tilde{u}_i(\theta, M^p, n).
\end{aligned} \tag{3}$$

The dimensionless functions $\tilde{\sigma}_{ij}(\theta, M^p, n)$ and $\tilde{\epsilon}_{ij}(\theta, M^p, n)$ and $I(n, M^p)$ (the latter is essentially constant for low mixity values) have been numerically determined by Shih [7] for $n = \frac{1}{3}$ and $n = \frac{1}{13}$. The dimensionless functions $\tilde{u}_{ij}(\theta, M^p, n)$ are derived in the Appendix from the strain functions and are shown in Fig. 2 for $n = \frac{1}{13}$.

Consider now the case shown in Fig. 5 where a shear band forms an angle $\phi$ with the crack direction. When the stresses directly ahead of the crack are unknown, but the relative far-field displacement is assumed to take place parallel to a single narrow shear band, we can determine the mixity parameter from the dimensionless function of the relative displacement field, since, from Fig. 5:

$$\tan\phi = \frac{u_\theta}{u_r} = \frac{\tilde{u}_\theta(\pi, M^p, n)}{\tilde{u}_r(\pi, M^p, n)}. \tag{4}$$

Figure 3 shows the variation of the mixity parameter with the angle $\phi$ for $n = \frac{1}{13}$. Thus, the angle $\phi$ determines the applicable dimensionless stress and strain functions.

The $J$ integral can be evaluated in terms of the shear strength $k$, the far field displacement

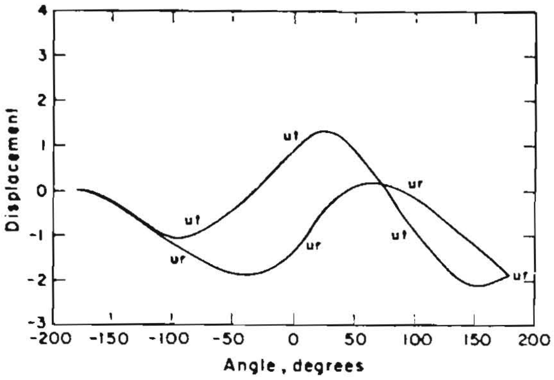


Fig. 2. Angular variation of the radial and tangential near tip dimensionless displacement functions for plane strain with $n = 1/13$ and $M^p = 0.5$.

$U$ and the crack-shear band angle $\phi$ (Fig. 5) by:

$$J = \frac{kU}{\cos\phi}. \tag{5}$$

The mean normal stress for the incompressible, plane strain plasticity is:

$$\sigma = \frac{\sigma_{rr} + \sigma_{\theta\theta}}{2}. \tag{6}$$

So from (3), the triaxiality is:

$$\sigma/\tau = \frac{\bar{\sigma}_{rr} + \bar{\sigma}_{\theta\theta}}{2\tau} \tag{7}$$

where

$$\bar{\tau} = \left[\bar{\sigma}_{r\theta}^2 + \left(\frac{\bar{\sigma}_{rr} - \bar{\sigma}_{\theta\theta}}{2}\right)^2\right]^{1/2}. \tag{8}$$

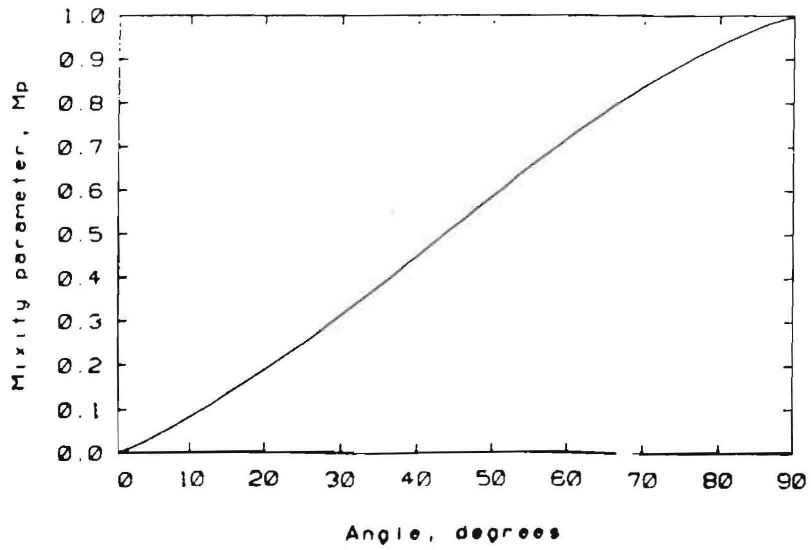


**Fig. 3. Mode I mixity parameter $M^p$ as a function of the crack-shear band angle $\phi$.**

The angular variation of the triaxiality, $\sigma/\tau$, for $n = \frac{1}{13}$, is shown in Fig. 4. Note that the triaxiality is highest for negative values of $\theta$ for all cases except pure Mode I.

Similarly, the dimensionless principal shear strain $\gamma$ can be expressed for the incompressible case as:

$$\bar{\gamma} = 2\left[\bar{\epsilon}_{r\theta}^2 + \left(\frac{\bar{\epsilon}_{rr} - \bar{\epsilon}_{\theta\theta}}{2}\right)^2\right]^{1/2} = 2\sqrt{\bar{\epsilon}_{r\theta}^2 + \bar{\epsilon}_{rr}^2}. \tag{9}$$

Solving (3) and (5) for the displacement and using (9), allows writing the far-field displacement in terms of the equivalent shear strain at any point in the near field:

$$U = \frac{\bar{\sigma}_1}{k} I(n, M^p)\, r\cos\phi\, (\gamma/\bar{\gamma})^{n-1}. \tag{10}$$

The displacement found from (10) is the critical displacement for crack initiation at the point $(r, \theta)$. The corresponding critical strain [which is used in (10)] is found by using the fracture criterion of McClintock, Kaplan and Berg [5] by which it is postulated that fracture due to micro-void coalescence occurs when a quantity $\eta$, named "damage," reaches a value of unity. The damage is expressed in terms of a hole growth ratio $F_t$, the principal shear strain $\gamma$ and the triaxiality $\sigma/\tau$.

$$\eta = \frac{1}{\ln F_t}\left[\ln\sqrt{1+\gamma^2} + \frac{\gamma}{2(1-n)}\sinh\left(\frac{(1-n)\sigma}{\tau}\right)\right]. \tag{11}$$

The crack is assumed to actually advance to the direction requiring the least far-field displacement to reach critical damage. Once the displacement for the critical point $(r_c, \theta_c)$ is known, the strain at all other points can be found by rearranging (10):

$$\gamma = \left[\frac{kU}{r\bar{\sigma}_1 I(n, M^p)\cos\phi}\right]^{1/(n-1)} \bar{\gamma}. \tag{12}$$

After crack initiation, the crack will grow such that each increment depends on the original crack initiation and all preceding crack growth increments. Differentiating (11) gives an expres-

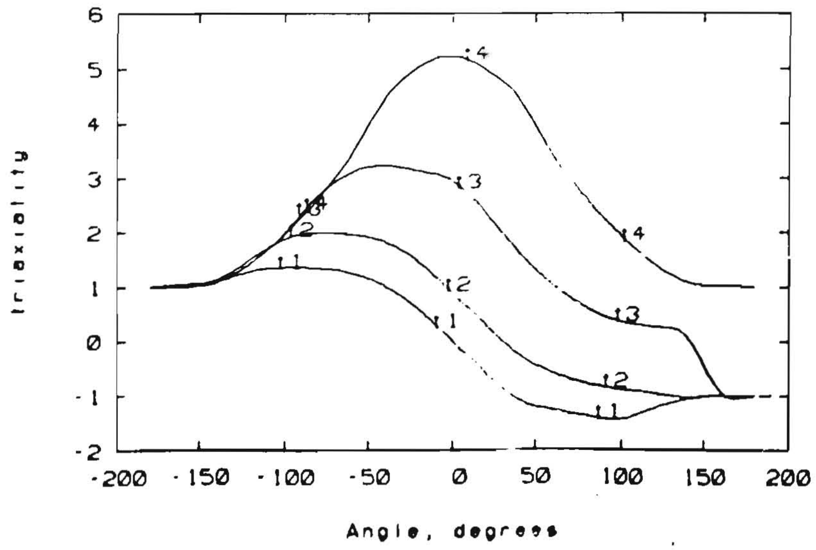


**Fig. 4. Angular variation of the triaxiality $\sigma/\tau$ for plane strain with $n$ = 1/13 and mixity $M^p$ = 0, 0.5, 0.82, 1.0 (corresponding to $t1$, $t2$, $t3$, $t4$).**

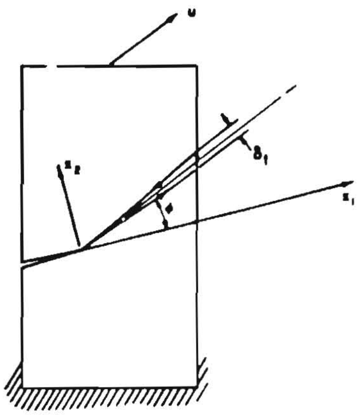

Fig. 5. *J*-integral parameters.

sion for the damage increments in terms of the strain increment and the strain itself:

$$d\eta = \frac{1}{\ln F_t}\left[\frac{\gamma}{1+\gamma^2} + \frac{1}{2(1-n)}\sinh\frac{(1-n)\sigma}{\tau}\right] d\gamma. \tag{13}$$

The strain increment can be found in terms of the far-field displacement increment by differentiating and rearranging (10):

$$d\gamma = \frac{\tilde{\gamma}k}{(n+1)\bar{\sigma}_1 I(n, M^P) r\cos\phi}(\tilde{\gamma}/\gamma)^n dU. \tag{14}$$

The damage at any point in front of the growing crack is given by the sum of the damage due to crack initiation [as found from (12) and (11)] and all of the damage increments from prior crack growth [as found from (13) and (14)]. At each increment the direction of the crack is taken as the average up to that point.

From the existing damage at a particular point, the necessary increment in damage for fracture is $\delta\eta = 1 - \eta$. The corresponding strain increment can be found from (13):

$$\delta\gamma = (1-n)\ln F_t \Big/ \left[\frac{\gamma}{1+\gamma^2} + \frac{1}{2(1-n)}\sinh\frac{(1-n)\sigma}{\tau}\right]. \tag{15}$$

The necessary increment in far-field displacement to cause this strain increment can be found from (14):

$$dU = (n+1)\frac{\bar{\sigma}_1 I(n, M^P) r\cos\phi}{\tilde{\gamma}k}(\gamma/\tilde{\gamma})^n d\gamma. \tag{16}$$

The crack will actually advance to the point which requires the least far field displacement to reach critical damage, not necessarily the most severely damaged site.

The equations above approach a singular Volterra integral equation and cannot be integrated in closed form; the crack orientation is not known in advance and also the functions ($\tilde{\ }$) are not known in closed form. Numerical procedures should be used. The damage is considered at points a distance $\rho + \delta c/2$ ahead of the crack tip (Fig. 6). When the critical direction is found, corresponding to the minimum displacement for unit damage, the crack is advancing by $\delta c$ to a point $\rho - \delta c/2$ from the critical point. At crack initiation, a Newton–Raphson technique is used to solve (11). Several sites are considered in front of the crack and the direction of crack advance is found by minimizing a parabola fitted to the critical displacement increments for these sites. During growth the accumulated damage due to crack initiation and prior incremental growth of the crack is calculated at each site and the necessary increment of displacement to

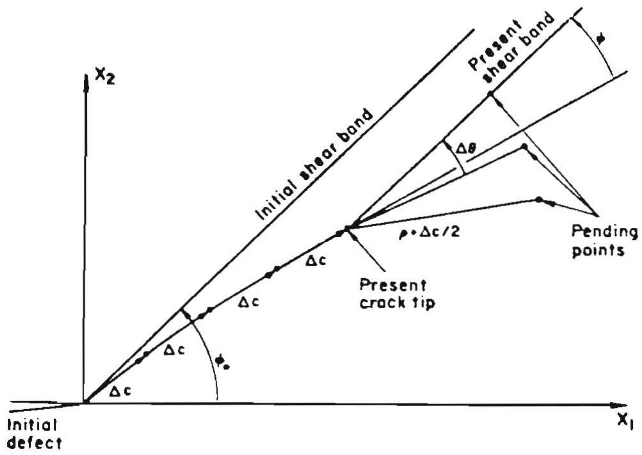


Fig. 6. Incremental crack growth.

reach damage of unity is found. Then the direction of minimum displacement increment is determined. Since the damage decreases rapidly with distance ahead of the crack tip, no accuracy is lost and large computation time savings are achieved by doubling continuously the intervals between crack growth sites (starting from the most recent one) when we consider the effect of prior crack growth. At each point of this last step, all quantities are calculated as if the crack was at the average direction (and not at that of the last increment) to better simulate the effect of prior growth. The above analysis was carried out with a well-annotated FORTRAN IV computer program. A substantial part of the programming was performed by Carter [1]. The program can be further developed to take into account cases like the existence of an inclusion at any site, the shape of an inclusion and the possibility of a breaking inclusion. Finally, there is need for a more detailed study, since, as was pointed out by Kardomateas and McClintock [2], the results associated with superimposing the stationary crack fields do not take into account the convection of hardened material.

## RESULTS OF THE INCREMENTAL MODEL

For a hole growth factor of $F_t$ = 1.3 and for a material with ratio of flow stress over shear yield $\bar{\sigma}_1/k$ = 3 and strain hardening $n = \frac{1}{13}$, Fig. 7 shows the crack path for an initial crack-shear band angle of $\phi_0$ = 45° where the normalized crack advance per step was taken as $\delta c/\rho = \frac{1}{8}$ and 50 sites with 1° spacing were considered around the tip at each step. The crack reaches a near steady direction of ~24° from the shear band as is seen also from Fig. 9 which shows the variation of the average crack direction. The corresponding Mode I mixity parameter

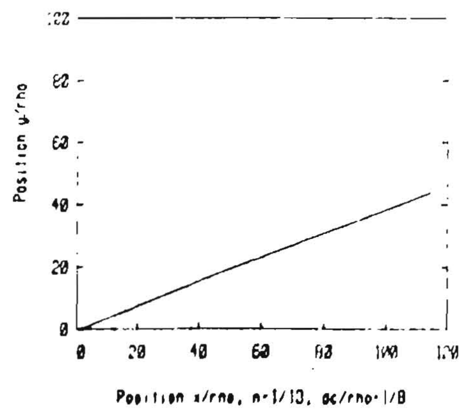


**Fig. 7. Growing crack path for an initial crack-shear band angle of $\phi_0$ = 45°.**

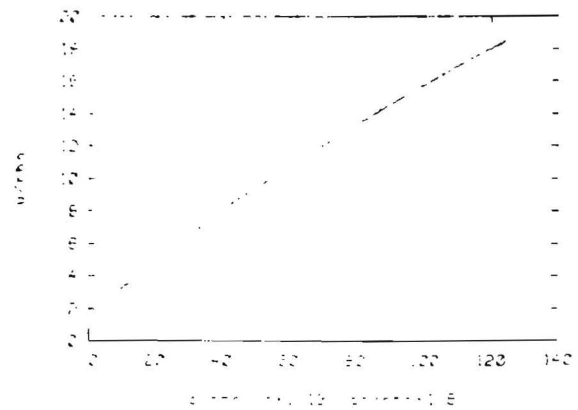

Fig. 8. Far-field displacement vs crack growth.

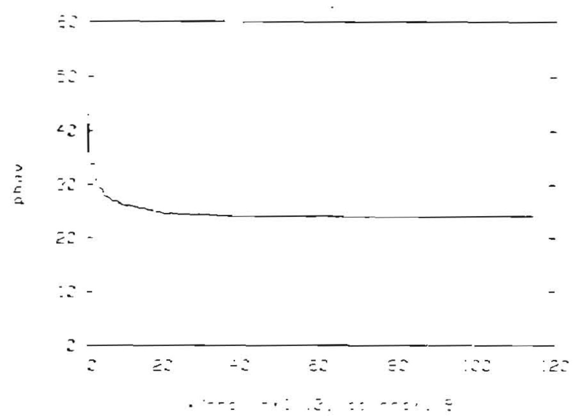

Fig. 9. Average crack-shear band angle vs projected crack advance.

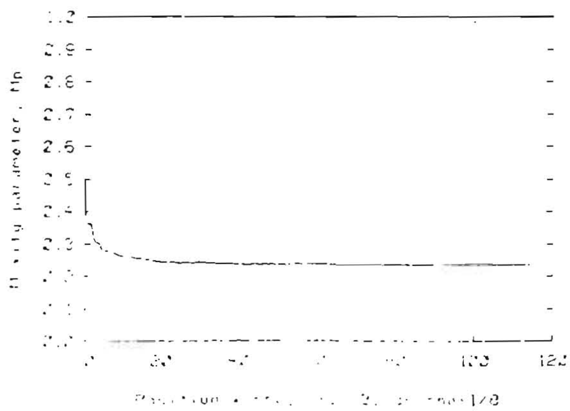

Fig. 10. Mode I mixity $M^p$ vs projected crack advance.

is about 0.23 instead of the initial 0.5 (Fig. 10). A plot of the crack growth vs far-field displacement is shown in Fig. 8. The crack initiation displacement (normalized with respect to the inclusion spacing) is $u_1/\rho = 0.79$ and we can see that the rate of crack growth ($dc/du$) increases with crack advance but the increase gets smaller as the crack grows. The average crack advance per unit displacement after growth by $c/\rho = 60$ is 27% bigger than the rate at $c/\rho = 20$. Further growth by the same amount (i.e. at $c/\rho = 100$) increases the crack growth rate only by 10% (as seen from Fig. 8). The critical strain for crack initiation was found $\gamma = 0.49$ and during subsequent growth it was (at the critical point) $\gamma = 0.77 + 0.07$ (Fig. 11).

The following conclusions were drawn after running the program for two strain hardening exponents, $n = \frac{1}{4}$ and $n = \frac{1}{13}$, and for initial crack-shear band angles $\phi_0$ of 0°, 22.5°, 45° and 65°.

(i) Larger strain hardening results in a smaller crack advance per unit displacement ($dc/du$) and a smaller critical strain at the growth points.

(ii) A smaller strain hardening causes the crack to come closer to the shear band, i.e. the average crack-shear band angle is smaller and the triaxiality is smaller.

(iii) For the low strain hardening $n = \frac{1}{13}$, increasing initial crack-shear band angles ($\phi_0$) gave smaller initiation displacements and strains and increasing crack growth rates ($dc/du$).

(iv) Strains and triaxialities during growth are relatively insensitive to the initial crack-shear band angle.

(v) For both strain hardening exponents and all the angles $\phi_0$, the final average shear band-crack growth angle $\phi_{avg}$ after growth by $c/\rho = 100$ was between 23° and 32°. The Mode I mixity corresponding to the final crack orientation was also within a narrow range for each of the strain hardening exponents. This shows a tendency of the growing crack to deviate from the shear band in a certain small angle range even with large initial shear band angles.

(vi) The results do not predict instability (infinite slope of the crack advance-far field displacement curve), which should, however, be coupled to the compliance of the surrounding structure.

(vii) A larger hole growth factor $F_r$ results in higher strains and initiation displacements but smaller crack growth rates ($dc/du$).

(viii) The displacement for initiation as related to the critical principal shear strain $\gamma_c$ and the mean inclusion spacing $\rho$ is of the order:

$$u_1/\rho = (1.6\text{–}2.1)\gamma_c \text{ for } n = \tfrac{1}{13}, \text{ and}$$
$$= (1.4\text{–}2.1)\gamma_c \text{ for } n = \tfrac{1}{4}.$$

(ix) The case $\phi_0 = 0°$ and $n = \frac{1}{13}$ gave initial normalized displacement $u_1/\rho = 1.08$ and an average steady crack-shear band angle of about 23° (with corresponding Mode I mixity $M_p = 0.22$) towards a region of higher triaxiality. The average crack growth rate for growth by $c/\rho = 120$ was $\Delta c/\Delta u \approx 6.56$. McClintock and Slocum's [6] approximate analysis in which the crack was assumed to propagate along the shear band (which is essentially a special case of

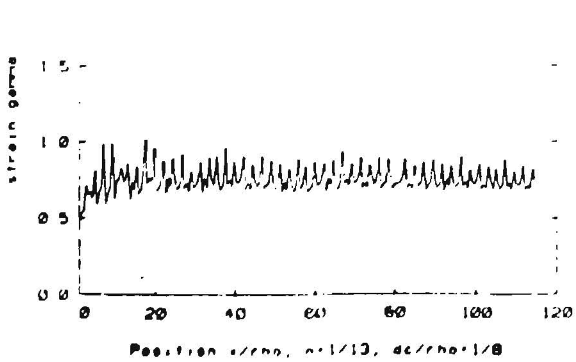


Fig. 11. Critical principal shear strain at the growth points.

**Table 1. Initiation conditions**

strain, triaxiality and displacement for initiation

| | n=1/13 | | | n=1/3 | | |
|---|---|---|---|---|---|---|
| | $\gamma$ | $\sigma/\tau$ | $u_1/\rho$ | $\gamma$ | $\sigma/\tau$ | $u_1/\rho$ |
| $\phi_0$= | | | | | | |
| 0 | 63 | 28 | 1 08 | 54 | 45 | 1 14 |
| 22 5 | 63 | 29 | 1 08 | 65 | 26 | 1 01 |
| 45 | 49 | 5 | 79 | 46 | 7 | 62 |
| 65 | 24 | 98 | 51 | 58 | 23 | 1 06 |

Table 2. Growth rate and crack orientation

Avg crack growth rate $c/\Delta u = c/(u-u_1)$
after growth by $c/\rho$=100

| | n=1/13 | n=1/3 |
|---|---|---|
| $\phi_0$= | | |
| 0 | 6.56 | 5 74 |
| 22.5 | 6.62 | 5 82 |
| 45 | 6.65 | 5 78 |
| 65 | 6.74 | 5 42 |

Average crack-shear band angle after growth by $c/\rho$=120

| | n=1/13 | n=1/3 |
|---|---|---|
| $\phi_0$= | | |
| 0 | 23 | 30 5 |
| 22 5 | 24.5 | 32 |
| 45 | 24 | 30 |
| 65 | 24.5 | 25 |

Table 3. Growth strain and mixity

Critical principal shear strain at growth sites

| | n=1/13 | n=1/3 |
|---|---|---|
| $\phi_0$= | | |
| 0 | .75±.07 | 61±.02 |
| 22 5 | .78±.06 | .61±.03 |
| 45 | .77±.07 | .65±.04 |
| 65 | .76±.06 | .67±.03 |

Mode I Mixity $M^p$ of the growing crack
(after growth by $c/\rho$=120)

| | n=1/13 | n=1/3 |
|---|---|---|
| $\phi_0$= | | |
| 0 | .22 | .19 |
| 22 5 | .24 | .19 |
| 45 | .23 | .19 |
| 65 | .20 | 15 |

the above for $M^p = 0$ and $\theta = 0$), gave bigger initial displacement ($u_1/\rho = 1.3$) and about 9% smaller crack growth rate. This indicates the importance of the effect of crack direction. The initiation strain was 12% smaller.

Tables 1–3 give some representative values for the strains, triaxialities and displacements, as derived by the above incremental analysis.

## CONCLUSIONS

A crack near a weld or a shoulder, loading into the plastic range, can give an asymmetric shear band extending from the crack tip. The resulting crack propagation into previously damaged material gives less ductility than the typical symmetric case. A computer program for predicting the crack growth has been developed using Shih's [7] asymptotic fields for a stationary crack in nonlinear elastic material under mixed mode loading. It outputs the conditions for crack initiation and growth (strain, triaxiality, displacement, crack growth rate, crack orientation). Cracking is assumed to occur at the point around the tip that needs the least far field displacement for critical damage. For a 45° shear band, it is found that the crack does not advance along the shear band but at an angle of about 24° under a higher triaxiality. Directional effects are therefore important; a higher crack growth rate is also predicted than if the directional effects are neglected and the crack is assumed to progress along the shear band. Strain hardening affects the crack growth rate, the critical strain at the growth points and the final steady direction of the growing crack. Strains and triaxiality during growth are not sensitive to the initial crack-shear band angle.

*Acknowledgments*—The authors acknowledge with thanks the support of the Office of Naval Research, Structural Mechanics Program, Code 432, Arlington, Virginia, Contract N0014-82K-0025, and are especially grateful to the project monitor Dr. Y. Rajapakse for his interest in this work.

## REFERENCES

[1] W. T. Carter, Incremental solution of asymmetric crack growth along a single fully plastic shear band. M. Sc. thesis, Department of Mechanical Engineering, M.I.T. (1983).
[2] G. A. Kardomateas and F. A. McClintock, On the fully plastic flow past a growing asymmetric crack and its relation to machining mechanics. *Res. Memo. 267*, Fatigue and Plasticity Lab., Department of Mechanical Engineering, M.I.T. (1983).
[3] F. A. McClintock, in *Fracture*. (edited by H. Liebowitz) (1971).
[4] F. A. McClintock and M. A. David (1980) Crack growth in an asymmetric band. Res. Memo. 247, Fatigue and Plasticity Lab., Department of Mechanical Engineering, M.I.T. (1980).
[5] F. A. McClintock, S. M. Kaplan and C. A. Berg, Ductile fracture by hold growth in shear bands. *Int. J. Fract. Mech.* **2**, 614–627 (1966).
[6] F. A. McClintock and A. H. Slocum, Predicting fully plastic Mode II crack growth from an asymmetric defect. accepted *Int. J. Fract. Mech.* (1983).
[7] C. F. Shih, Small scale yielding analysis of mixed mode plane strain crack problems. *Fracture Analysis, ASTM STP 560*, pp. 187–210. Am. Soc. Test. Mat., Philadelphia (1974).

(*Received* 13 *July* 1984; *received for publication* 11 *September* 1984)

### APPENDIX—DISPLACEMENT FUNCTIONS

The dimensionless displacement functions $u_i$ will now be determined from the strain functions. For plane strain, the radial displacement $u_r$ may be found from

$$\epsilon_{rr} = \frac{\partial u_r}{\partial r}, \tag{17}$$

so:

$$u_r = \int_0^r \epsilon_{rr} \mathrm{d}r - f(\theta). \tag{18}$$

The boundary condition that the radial displacement is zero at $r = 0$ for all angles gives $f(\theta) = 0$. Eliminating $\epsilon_{rr}$ with (3) and integrating:

$$\frac{u_r}{r} = \left[\frac{J}{\bar{\sigma}_1 r I(n, M^p)}\right]^{1/(n+1)} \left(\frac{n+1}{n}\right) \epsilon_{rr}. \tag{19}$$

and using again (3) we determine the radial displacement function $u_r$ with respect to the displacement at $\theta = -\pi$:

$$\tilde{u}_r(\theta, M^p, n) = \frac{n+1}{n}(\tilde{\epsilon}_{rr}(\theta, M^p, n) - \tilde{\epsilon}_{rr}(-\pi, M^p, n)). \tag{20}$$

The dimensionless tangential displacement function $u_\theta$ is determined from

$$\epsilon_{\theta\theta} = \frac{1}{r}u_r + \frac{1}{r}\frac{\partial u_\theta}{\partial \theta} \tag{21}$$

as:

$$u_\theta = \int_{-\pi}^{\theta} (r\epsilon_{\theta\theta} - u_r)d\theta + f(r). \tag{22}$$

Noting that $\epsilon_{rr} = -\epsilon_{\theta\theta}$ for plane strain incompressibility and using (3) with (20) gives the tangential displacement:

$$\frac{u_\theta}{r} = -\left[\frac{J}{\bar{\sigma}_1 r I(n, M^p)}\right]^{1/(n+1)}\left(\frac{2n+1}{n}\right)\int_{-\pi}^{\theta} \tilde{\epsilon}_{rr}d\theta + f(r). \tag{23}$$

With respect to the displacement at $\theta = -\pi$, $f(r) = 0$. By using (3) we can thus find the dimensionless tangential displacement function relative to the displacement at $\theta = -\pi$, in terms of the dimensionless strain function $\tilde{\epsilon}_{rr}$:

$$\tilde{u}_\theta(\theta, M^p, n) = -\frac{2n+1}{n}\int_{-\pi}^{\theta} \tilde{\epsilon}_{rr}(\theta, M^p, n)d\theta. \tag{24}$$

Plots of the displacement functions, determined numerically by (24), (20) are given in Fig. 2.